DYNA
http://dyna.medellin.unal.edu.co/

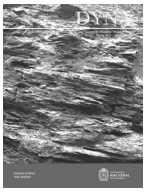

UNIVERSIDAD NACIONAL DE COLOMBIA

Influence of quenching and annealing heat treatments on the strain hardening properties of AISI steels: a statistical approach

Ricardo Andrés García-León [a]*, Haidee Yulady Jaramillo [b] & July Gómez-Camperos [b]

[a] *Programa de ASST, Universidad del Magdalena, Santa Marta, Colombia. *: ragarcial@ufpso.edu.co*
[b] *Mechanical and Civil Engineering Department, Engineering Faculty. Universidad Francisco de Paula Santander Ocaña, Colombia. hyjaramillo@ufpso.edu.co, jagomezc@ufpso.edu.co*

Received: October 29th, 2024. Received in revised form: December 6th, 2024. Accepted: December 16th, 2024.

Abstract
The knowledge of the stress-strain curve is of great interest due to the different parameters, conditions, and applications to which materials are exposed in different industrial sectors. This statistical study aims to analyze the strain-hardening behavior of two AISI-grade materials (1045 and 304). The ASTM E-8 standard procedure guidelines were considered for different hardening percentages due to plastic deformation (20% and 40%), following an experimental design of 45 tests, including repetitions. The results revealed an improvement in the material's mechanical properties corresponding to the hardening percentage, which was also correlated with the heat treatment process. Finally, response surface methodology plots were generated, depicting predictive equations governing the behavior of the response variables (stress, yield, load, and strain) with a confidence level of 98% in the results.

Keywords: strain hardening; statistical analysis; prediction; RSM

Influencia de los tratamientos térmicos de temple y recocido en las propiedades de endurecimiento por deformación de los aceros AISI: un enfoque estadístico

Resumen
El conocimiento de la curva esfuerzo-deformación es de gran interés debido a los diversos parámetros, condiciones y aplicaciones a las que se ven expuestos los materiales en diferentes sectores industriales. Este estudio estadístico tiene como objetivo analizar el comportamiento de endurecimiento por deformación de dos materiales grado AISI (1045 y 304). Se consideraron los lineamientos de procedimiento de la norma ASTM E-8 para diferentes porcentajes de endurecimiento por deformación plástica (20% y 40%), siguiendo un diseño experimental de 45 ensayos, incluyendo repeticiones. Los resultados revelaron una mejora en las propiedades mecánicas del material correspondiente al porcentaje de endurecimiento, el cual también se correlacionó con el proceso de tratamiento térmico. Finalmente, se generaron gráficos de la metodología de superficie de respuesta, representando ecuaciones predictivas que gobiernan el comportamiento de las variables de respuesta (esfuerzo, fluencia, carga y deformación) con un nivel de confianza del 98% en los resultados.

Palabras clave: endurecimiento por deformación; análisis estadístico; predicción; RSM.

1 Introduction

The machine elements design relies heavily on a comprehensive understanding of materials' mechanical and microstructural behavior. During both manufacturing and operational use, materials are exposed to different factors, such as temperature fluctuations and mechanical loads. These conditions induce stresses that can significantly modify the materials' mechanical and physical properties [1]. Strain hardening is a critical phenomenon for many industrial alloys. It occurs when a material is subjected to plastic deformation, increasing its resistance to further deformation. This property is especially

How to cite: García-León, R.A., Jaramillo, H.Y., and Gómez-Camperos, Y., Influence of quenching and annealing heat treatments on the strain hardening properties of AISI steels: a statistical approach. DYNA, 92(235), pp. 38-46, January - March, 2025.

important in industries that manufacture parts and components subject to high stress, as it can enhance durability and performance [2].

Patiño-Perez *et al.* [3] evaluated the AISI 1006 alloy using different suppliers to determine its elongation and thinning properties according to ASTM standards. Salman [4] explored the microstructure and mechanical properties of AISI 1018 low-carbon steel subjected to a cold rolling process. Dimatteo *et al.* [5] developed a prediction model for strain-hardening behavior in multiphase steels. Bounezour *et al.* [6] investigated the effects of strain hardening on the mechanical properties of two metallic materials (XC38 steel and aluminum alloy).

Using simulations and experiments, Eom et al. [7] compared the plastic deformation behavior of pre-heat-treated steel (PHTS) and SCM435 steel. PHTS exhibited a high initial yield strength and negligible strain-hardening capacity, while SCM435 exhibited good strain-hardening behavior under the experimental conditions evaluated. Pérez *et al.* [8] analyzed the conditions of quenching and annealing heat treatments and their impact on the mechanical properties of hardness, toughness, and mechanical strength of 5160H steel. Lorenzo *et al.* [9] investigated the mechanical behavior of two different steels under cyclic loading, focusing on the Bauschinger effect and hardening rule, which better represent the material's plastic behavior. Using analysis of variance, Soria Aguilar et al. [10] studied the impact of two cycles on the microstructure and mechanical properties of API-5CT-J55 welded steel.

Considering the above, this study addresses a significant gap in the current literature by investigating the effects of thermal annealing treatments, specifically quenching and annealing, on AISI 1045 and 304 steels subjected to different strain-hardening conditions, with the aim to analyze the influence of treatment parameters and response variables statistically. While previous research has examined various heat treatments and their impact on mechanical properties, detailed insights into how these treatments affect strain-hardening behavior and corresponding mechanical performance across different geometries remain limited. The scientific challenge lies in accurately modeling and predicting the mechanical behavior of these steels under the combined effects of strain hardening and heat treatment [2].

2 Materials and methods

The methodology developed in this research is shown in Fig. 1, based on 5 steps. Initially, circular bar samples of hot-rolled AISI 1045 and 304 steel were selected, considering the guidelines of the ASTM E-8. These materials were in the hot-rolled state, which introduces anisotropy due to the rolling process.

2.1 Experimental design

Initially, for the factorial design, it was necessary to consider the parameters (input variables) and the response variables (output), as shown in Table 1. The factorial design type used was the fractional Box-Behnken design, which allows for evaluating a fraction of all possible

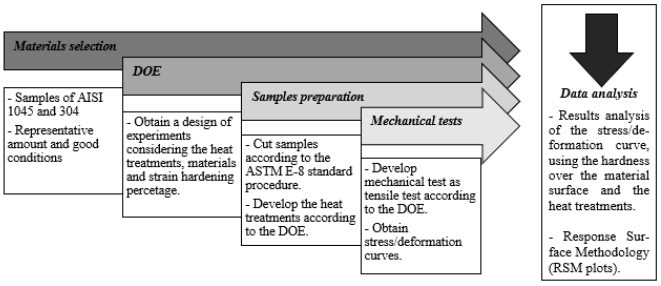

Figure 1. Methodology applied to this work. Note: DOE, design of experiments. Source: The authors.

Table 1.
Specification of parameters and response variables

Parameters	ID	Level	Response variables	ID
Steel	AISI 1045	27 samples	Yield strength	YS
	AISI 304	18 samples	Tensile strength	UTS
Heat treatment (HT)	Original-O	-1	Unit strain	Unit def.
	Quenched-T	0	Maximum load	CM
	Annealed - R	1	Strain hardening capacity	SHc
Strain hardening percentage (SH%)	0%	-1	---	---
	20%	0	---	---
	40%	1	---	---

Source: The authors.

combinations (3^3 design). This approach involves selecting a subset of the combinations and conducting experiments only with those combinations, optimizing the study of the variables' effects efficiently. Note that a total of 45 samples of both materials were used.

2.2 Quenching and Annealing heat treatments

For AISI 1045 steel in the quenching treatment, the steel was preheated to a temperature of 850°C for 30 min and then cooled in water. For the annealing treatment, the steel was heated to a temperature of 850°C for 60 min and then slowly cooled in the muffle furnace (Pinzuar equipment). Similarly, AISI 304 steel in the annealing treatment was heated at a temperature of 1,100°C for 30 min, followed by rapid cooling in water. As mentioned, due to the similar phase transformation during quenching and annealing, only annealing was carried out for the AISI 304 steel samples [11]. Annealing is a heat treatment process in which the material is heated to a temperature that "transforms into austenite and is then slowly cooled (down to 500°C)". As a result, the austenite transforms into coarse-grained pearlite and ferrite and then air-cooled [12].

2.3 Tensile test

The tensile tests were conducted using a Pinzuar/50K Universal Testing Machine in uniaxial direction along the sample longitudinal axis (Y-axis), which corresponds to the rolling direction of the hot-rolled steel bars, at a room

temperature of 23°C and 49% relative humidity, following the specifications (dimensions and geometry) of the ASTM-E8M standard procedure [13]. The sample machining precision and consistent cross-sectional dimensions are critical factors in obtaining reliable mechanical properties. Variations in these factors can significantly impact the tensile test results and other mechanical evaluations. The geometric data of the samples suggested for the tensile test were input into the equipment's software considering a calibrated length of 187.5 mm, a diameter of 12.5 mm, and a total length (300 mm). Note that the steel samples were machined using a machining center to guarantee the same circular geometry, where G: Calibrated length = 62.5 mm, D: Diameter = 12.5 mm, R: Fillet radius = 10 mm, and A: Reduced section length = 172.7 mm.

2.4 Strain hardening percentages (SH%)

In this process, the stresses and strains in the strain-hardening region were estimated to evaluate the different steels in their original state. The required stresses were obtained from [14]. Notably, hardness and yield strength increase more than tensile strength, especially in the initial deformation stage (10%) [15]. Also, the strain hardening capacity (SHc) can be estimated using Eq. 1, which was proposed by [16], taking into account the material mechanical parameters such as ultimate tensile strength (σ_{ult}) and yield strength (σ_y).

$$SHc = \frac{\sigma_{ult}}{\sigma_y} - 1 \quad (1)$$

2.5 Response surface methodology (RSM)

The statistical approximation of the wear test parameters such as steel (S), heat treatment (HT), and strain hardening percentage (%SH) on the response variables, which are yield strength (YS), tensile strength (UTS), unit deformation, maximum load and strain hardening capacity (SHc) were estimated. As a product of the combination of factors S, HT, and SH with 2 and 3 levels each one, respectively, 45 tests were developed for each steel in a Completely Randomized Design (CRD) with 3 replicate tests to guarantee the statistical dispersion of the results. These experiments aim to represent many factors and levels primarily responsible for the differences in the response. These contours showed a range of colors where blue is the minimum value and red is the maximum value for each plot obtained for the response variables using *Statgraphics* statistical software [17].

Response surface methodology (RSM) is a statistical technique to develop, improve, and optimize processes. It uses quantitative data from appropriate experiments to determine regression model equations and operating conditions [18]. The goal is to identify the relationships between response and input variables. Analyzing the surfaces can determine the optimal conditions for achieving desired mechanical properties in materials to facilitate better design and process control in material engineering.

2.6 Analysis of variance (ANOVA or AV)

An analysis of variance was performed on the evaluated parameters and response variables on the strain hardening behavior using the Statgraphics statistical software for the sources of variation (M, HT, and %SH) and their interactions [19]. AV is a statistical technique that analyzes the variation on the experimental results of a particular design, decomposing it into independent sources of variation attributable to each of the effects (variables) that constitute the experimental design [20]. In this statistical analysis, the factor's effects were analyzed, allowing the comparison of more than two levels simultaneously and determining whether there is a relationship between them and, thus, the positive or negative significance of the response variables. The significant or non-significant model terms were identified through the P index values, existing a significant effect between the factors, with P values equal to or less than 0.05 (P≤0.05).

3 Results and discussions

3.1 Experimental results for the RSM

Table 2 presents the mechanical properties of average values and their behavior, analyzed from the stress-strain curves obtained in the tensile tests for the entire experimental set (original samples). However, SHc was calculated using Eq. 1. Fig. 2 was obtained from both materials' tensile tests (stress-strain curves) based on the developed heat treatments.

The mechanical properties behavior of AISI 1045 and AISI 304 stainless steels after heat treatments and variations in strain hardening (SH) are according to the technical literature [21]. For AISI 1045, the quenching heat treatment (T-HT) significantly increases the yield strength (YS) and ultimate tensile strength (UTS), reaching up to 830.14 MPa and 1,055.26 MPa, respectively, for 40% SH. This steel also decreases maximum unit deformation and maximum load, making it more material brittle but stronger [22]. For the annealed heat treatment (R-HT) AISI 1045, the yield strength and ultimate tensile strength are lower than quenched samples but still higher

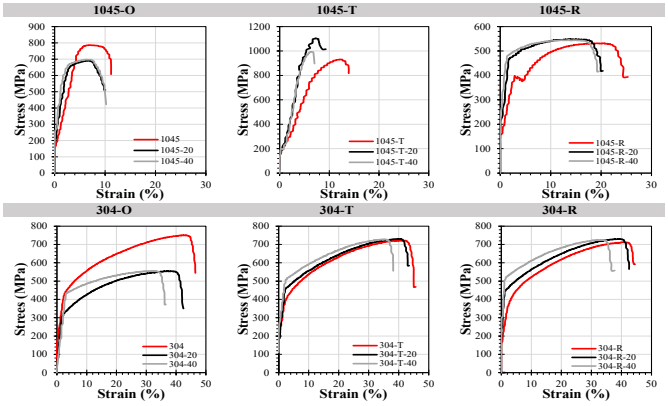

Figure 2. Stress-strain curves of AISI grade steels (1045-304).
Source: The authors.

Table 2.
Average mechanical properties analyzed from the stress-strain curves of AISI 1045 grade steels (O, T, and R) and AISI 304 (O and R), along with their corresponding SH variations (20 and 40%).

Parameters			Response variables				
Steel	HT	SH (%)	YS (MPa)	UTS (MPa)	Unit deformation (mm)	Max Load (kN)	SHc
AISI 1045	O	0	376.18	673.07	10.12	97.20	0.789
		20	563.09	698.75	9.213	86.03	0.241
		40	607.89	724.64	8.481	85.10	0.192
	T	0	700.00	943.22	13.22	122.90	0.347
		20	750.70	964.40	7.227	118.35	0.285
		40	830.14	1,055.26	6.893	115.16	0.271
	R	0	398.00	533.01	23.30	71.16	0.339
		20	493.55	563.2	19.60	62.23	0.141
		40	452.24	541.08	18.75	66.40	0.196
AISI 304	O	0	230.01	504.58	49.06	72.98	1.194
		20	302.17	538.36	42.33	66.06	0.782
		40	385.08	557.20	34.37	64.51	0.447
	R	0	220.62	444.16	53.74	61.61	1.013
		20	391.03	482.50	42.82	59.55	0.234
		40	386.46	478.34	39.39	52.98	0.238

Note: Where, SH is the strain hardening, and SHc is the strain hardening capacity.
Source: The authors.

than the original state (O), reflecting a more ductile and relaxed structure due to the formation of larger grains. Variations in SH% also show a decreasing trend in strain hardening capacity (SHc), with values decreasing from 0.339 in the original state to 0.196 at 40% SH, which aligns with greater energy absorption capacity and increased ductility. In AISI 304 stainless steel, strain hardening significantly increases the yield strength and ultimate tensile strength, with YS reaching 385.08 MPa and UTS reaching 557.20 MPa for 40% SH in the original state. This behavior is typical of austenitic steels exhibiting a high strain-hardening capacity. The annealing treatment (R) also improves ductility, but the increases in YS and UTS are less pronounced than in AISI 1045, reflecting its more ductile and tough nature [23].

3.1 Statistical results

3.2.1 ANOVA results

The response variables behavior of YS, UTS, Unit Def., Max. Load, and SHc were evaluated for both materials using the results in Table 4. The sum of squares (SS), F factor, and P values were also used to interpret statistical significance. Furthermore, the correlation coefficients R^2, MAE (Mean Absolute Error), and the Durbin-Watson statistic were used to assess the quality of the models, as shown in Tables 7 and 8 for the two steels.

Table 3 shows that, for the AISI 1045 analysis, heat treatment (HT) significantly impacts the properties of UTS and Max. Load, with P-values of 0.0119 and 0.0009, respectively, indicating strong statistical significance. It also affects Unit Def. with a P-value of 0.0023, suggesting strong significance. However, YS and SHc are unaffected (P-values of 0.0846 and 0.1690, respectively). Strain hardening (SH) significantly affects the response variables YS, Unit Def., and Max. Load, with P-values of 0.0138, 0.0363, and 0.0164, respectively, indicating strong statistical significance. However, the effects on UTS and SHc are insignificant (P-values of 0.1326 and 0.0740, respectively). This behavior indicates that strain hardening has a major impact on these properties.

Notice that AA interaction significantly affects all response variables except SHc, with extremely low P-values for YS, UTS, Unit Def., and Max. Load (0.0012, 0.0006, 0.0102, and 0.0001, respectively). This interaction does not significantly affect SHc (P-value of 0.8719). For AB Interaction, no significant effects were observed on any of the response variables, with high P-values across the board (all P-values > 0.1). However, BB interaction shows a trend towards significance for Max. Load with a P-value of 0.0659, while other variables are not significantly affected (P-values > 0.1). For model quality assessment, high R^2 values (YS: 98.44%, UTS: 98.87%, Unit Def.: 97.97%, Max. Load: 99.70%, SHc: 84.42%) indicate a good fit of the models to the data, suggesting that the variations in response variables are well-explained by the factors considered [23].

Pareto plots show the percentage contribution of each factor to the total variation in the mechanical properties, as was observed in Fig. 3.

Table 4 shows that for the AISI 304 analysis, HT significantly affects UTS and Max. Load, with P-values of 0.0010 and 0.0080, respectively, indicating strong statistical significance. It also affects SHc with a P-value of 0.0669, suggesting a trend toward significance. However, YS and Unit Def. are unaffected (P-values of 0.4244 and 0.0895). SH significantly affects all response variables. YS, UTS, Unit Def., Max. Load and SHc show strong statistical significance with P-values of 0.0115, 0.0040, 0.0018, 0.0117, and 0.0062, respectively. This behavior indicates that strain hardening has a major impact on these mechanical properties [24].

Table 3.
Analysis of Variance for AISI 1045.

Fuente	DOF	YS			UTS			Unit Def.			Max. Load			SHc		
		SS	F	P-Value	SS	F	P-Value	SS	F	P-Value	SS	F	P-Value	SS	F	P-Value
A:HT	1	6893.23	6.46	0.0846	35139.5	30.11	0.0119	190.812	95.57	0.0023	782.955	185.67	0.0009	0.049686	3.25	0.1690
B:SH	1	28855.1	27.04	0.0138	4912.34	4.21	0.1326	26.1084	13.08	0.0363	100.86	23.92	0.0164	0.110976	7.27	0.0740
AA	1	155074	145.31	0.0012	266939	228.71	0.0006	67.2181	33.67	0.0102	3326.56	788.84	0.0001	0.000470	0.03	0.8719
AB	1	7873.90	7.38	0.0728	473.062	0.41	0.5696	2.11848	1.06	0.3788	13.4689	3.19	0.1719	0.051529	3.37	0.1635
BB	1	3478.61	3.26	0.1688	17.1698	0.01	0.9111	4.18955	2.10	0.2433	33.8939	8.04	0.0659	0.035555	2.33	0.2244
Error total	3	3201.61	---	---	1167.16	---	---	1.99657	---	---	4.217	---	---	0.015269	---	---
Total (corr.)	8	205377	---	---	310983	---	---	296.437	---	---	4270.39	---	---	0.294026	---	---
R^2	-	98.44%			98.87%			97.97%			99.70%			84.42%		
MAE	-	16.61			16.90			0.68			1.01			0.06		
Durbin-Watson	-	3.46091 (P=0.9091)			2.04502 (P=0.2033)			2.19018 (P=0.2608)			3.4441 (P=0.9028)			2.08344 (P=0.2177)		

Where: SS, sum of squares, DOF, degrees of freedom.
Source: The authors.

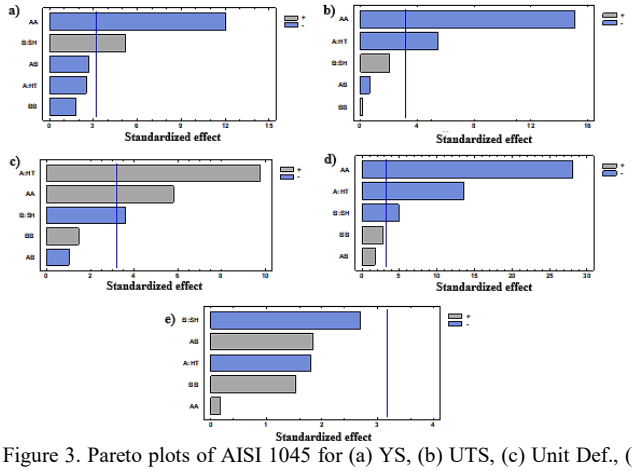

Figure 3. Pareto plots of AISI 1045 for (a) YS, (b) UTS, (c) Unit Def., (d) Max. Load, and (e) SHc.
Source: The authors.

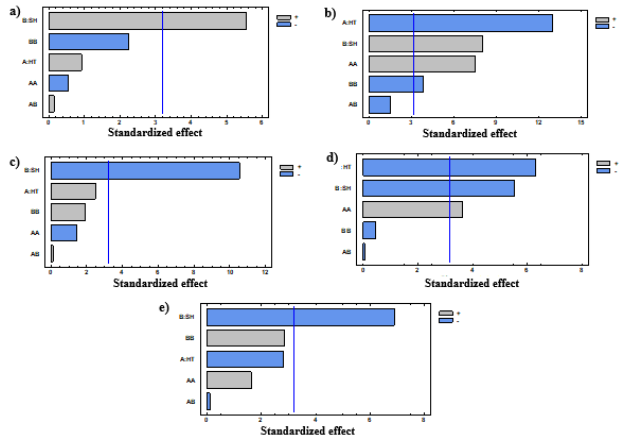

Figure 4. Pareto plots of AISI 304 for (a) YS, (b) UTS, (c) Unit Def., (d) Max. Load, and (e) SHc.
Source: The authors.

Notice that AA interaction shows significant effects on UTS and Max. Load with extremely low P-values (0.0049 and 0.0356 respectively). This interaction also affects SHc (P-value of 0.2024), suggesting some influence. However, the effects on YS and Unit Def. are insignificant (P-values of 0.6313 and 0.2480, respectively). For AB interaction, no significant effects were observed on any of the response variables, with high P-values across the board (all P-values > 0.2). However, BB interaction significantly affects UTS and SHc with P-values of 0.0311 and 0.0652, respectively. Other variables are not significantly affected (P-values > 0.1) [25]. For model quality assessment, high R2 values for most variables (YS: 92.50%, UTS: 97.26%, Unit Def.: 96.54%, Max. Load: 95.67%) indicate a good fit of the models to the data, suggesting that the variations in response variables are well-explained by the factors considered. However, the R2 value for UTS (9.03%) suggests that the model does not explain much of the variability in this response variable.

Pareto charts show that the variables B:SH and A:HT are the most frequent for all analyzed variables, as is shown in Fig. 4.

3.2.2. RSM plots

Fig. 5 shows the RSM plots for the AISI 1045 response variables, according to the statistical statements made in Table 3. Notice that YS increases significantly with higher levels of SH (Fig. 5a).

At the highest SH values (around 1 on the scale), YS reaches values close to 770 MPa. The influence of HT is also notable, with an intermediate level of HT contributing to higher YS values. However, high or low HT levels do not reach the maximum YS. From Fig. 5b, UTS shows a steady increase with HT and SH. Higher levels of SH (approaching 1) and higher HT levels result in UTS values near 1,120 MPa. This behavior suggests that both parameters should be optimized to maximize ultimate strength. Unit Def. behavior decreases as SH

Table 4.
Analysis of Variance for AISI 304.

Fuente	DOF	YS			UTS			Unit Def.			Max. Load			SHc		
		SS	F	P-Value	SS	F	P-Value	SS	F	P-Value	SS	F	P-Value	SS	F	P-Value
A:HT	1	1089.45	0.85	0.4244	6346.60	168.90	0.0010	17.3060	6.14	0.0895	144.158	39.87	0.0080	0.146641	7.93	0.0669
B:SH	1	39487.6	30.83	0.0115	2439.36	64.92	0.0040	313.782	111.29	0.0018	110.339	30.51	0.0117	0.879368	47.58	0.0062
AA	1	363.151	0.28	0.6313	2115.53	56.30	0.0049	5.76867	2.05	0.2480	48.0527	13.29	0.0356	0.048880	2.64	0.2024
AB	1	28.9982	0.02	0.8899	85.0084	2.260	0.2296	0.02890	0.01	0.9257	0.00641	0.00	0.9691	0.000196	0.01	0.9245
BB	1	6392.41	4.99	0.1116	554.889	14.77	0.0311	10.5035	3.73	0.1491	0.74013	0.20	0.6817	0.149969	8.11	0.0652
Error total	3	1280.84	---	---	37.577	---	---	2.81945	---	---	3.61606	---	---	0.018482	---	---
Total (corr.)	8	51204.1	---	---	11654.1	---	---	355.847	---	---	314.144	---	---	1.2805	---	---
R^2	-	92.50%			9.03%			97.26%			96.54%			95.67%		
MAE	-	18.34			3.06			0.86			0.97			0.069		
Durbin-Watson	-	3.21647 (P=0.7769)			3.03962 (P=0.6737)			3.26739 (P=0.8046)			3.25774 (P=0.7994)			3.22803 (P=0.7833)		

Where: SS, sum of squares, DOF, degrees of freedom, and MAE, Mean absolute error.
Source: The authors.

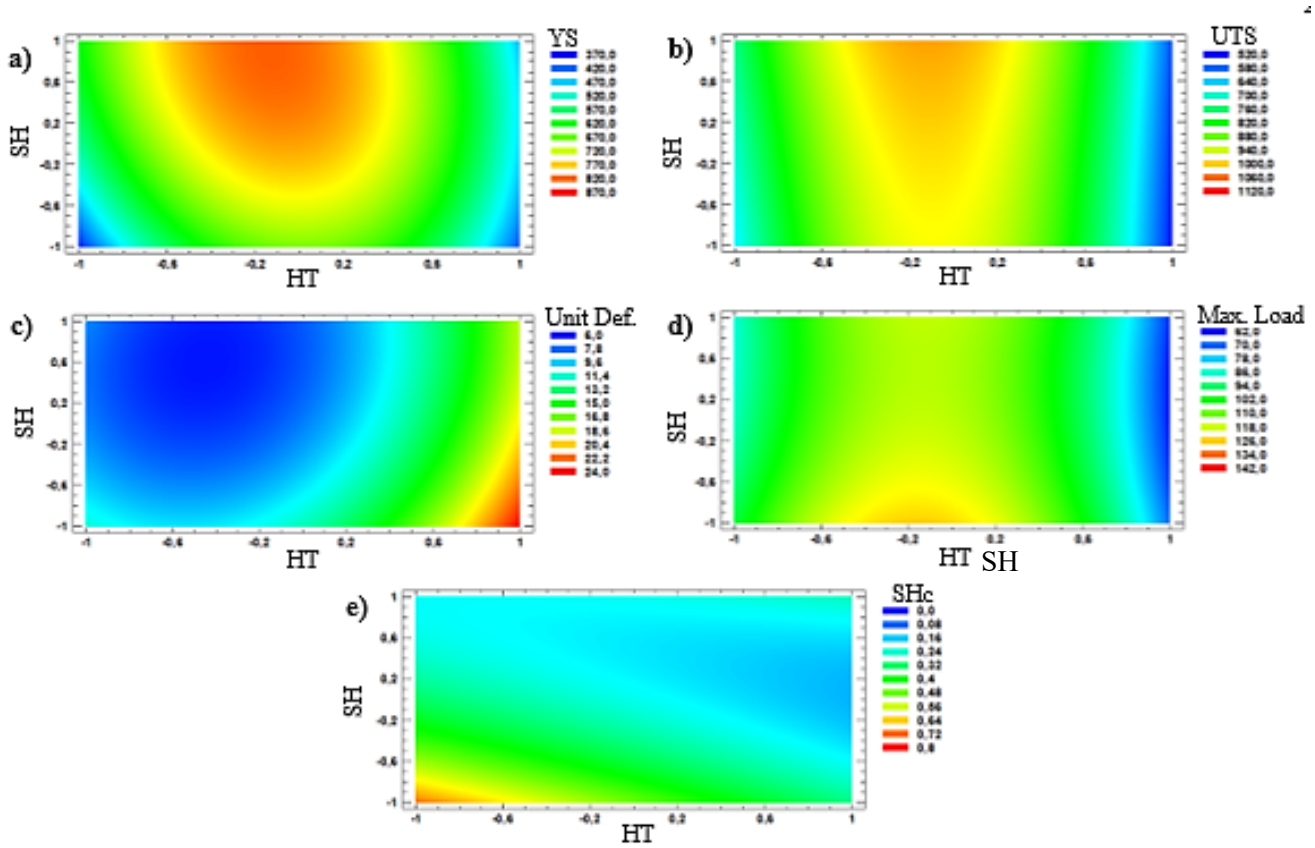

Figure 5. RSM plots for the AISI 1045 response variables.
Source: The authors.

increases, as shown in Fig. 5c. Note that the lowest deformation (around 8 mm) occurs at the highest SH levels. HT has a minimal impact compared to SH. These results indicate that increasing SH is more effective for reducing unit deformation. HT and SH influence the maximum load capacity, but SH has a more pronounced effect (See Fig. 5d). The highest maximum load (around 142 kN) is achieved with high SH and intermediate HT levels. Like YS, very high

or low HT levels are less effective than moderate levels. Finally, in Fig. 5e the strain-hardening capacity (SHc) increases significantly with higher SH levels, reaching values close to 0.86. HT has a lesser impact on SHc. Therefore, increasing SHc is crucial to enhance SHc.

Fig. 6 response surfaces include a detailed interpretation of each response surface about the color scale and corresponding numerical values. Fig. 6a for YS indicates that increasing %SH positively impacts the yield strength. The highest values of YS (440 MPa) are observed when %SH is around 1 and HT is between -0.6 to 0.4. Conversely, the lowest values of YS (200 MPa) are found at lower %SH and HT values near -1. This behavior suggests that heat treatment and strain hardening contribute significantly to increasing yield strength, with strain hardening having a more pronounced effect. The UTS response surface in Fig. 6b shows a moderate increase in ultimate tensile strength with increasing %SH and HT. The maximum value (680 MPa) is achieved at %SH around -0.2 and HT near 0.8. The minimum value (400 MPa) is observed at low %SH and HT values, which indicates a combined effect of HT and %SH on ultimate tensile strength, where optimized conditions can substantially enhance UTS. The response surface for Unit Def. illustrates that higher %SH and intermediate HT levels decrease unit deformation, with the minimum value (34 mm) appearing at %SH around 1 and HT at 0.6 as is shown in Fig. 6c. The maximum deformation (64 mm) is seen at low %SH and HT values. This behavior implies that strain hardening reduces unit deformation, improving material ductility. For the case of the Max. Load (See Fig. 6d), the response surface reveals that both %SH and HT positively influence the maximum load capacity. The highest load (77.6 kN) is observed at %SH near 1 and HT around 0.4. The lowest load (54.4 kN) is found at low %SH and HT values, which suggests that enhancing %SH and applying suitable heat treatment can significantly increase the material's load-bearing capacity. Finally, in Fig. 6e, the SHc response surface indicates that %SH strongly affects the strain hardening coefficient. The maximum SHc value (1.6) is achieved at %SH near 1 and HT around -0.4. The minimum SHc value (0.5) is seen as a low %SH and HT values. This result highlights that strain hardening predominantly influences the strain hardening coefficient, with heat treatment playing a secondary role.

Equations 2 to 6 describe the behavior of YS, UTS, unit def., max. load, and SHc under different experimental conditions for AISI 1045 steel. For AISI 304 steel, these properties are represented by equations 7 to 11. These equations enable the determination of specific values on the response surface about the material's mechanical properties.

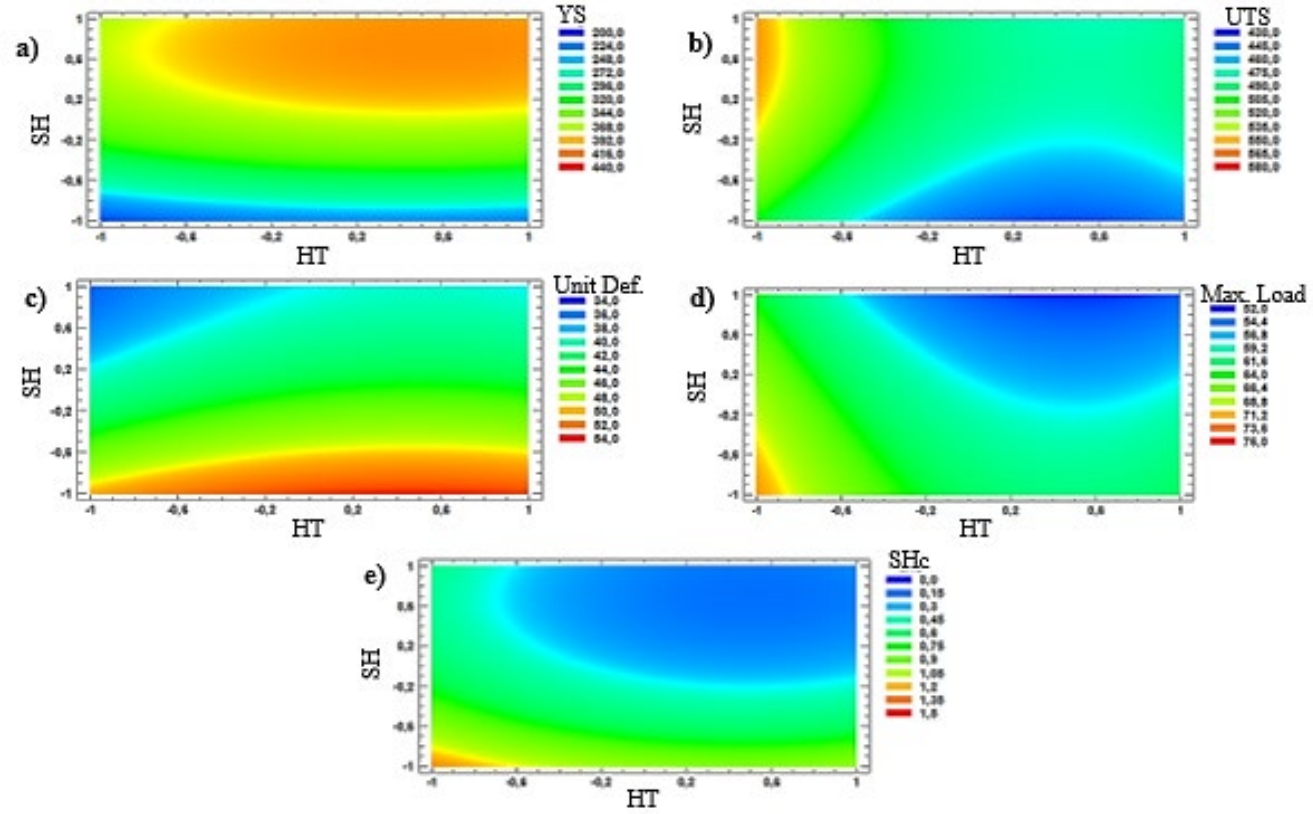

Figure 6. RSM plots for the AISI 304 response variables.
Source: The authors.

$$YS = 788.083 - (33.895 \times HT) + (69.3483 \times SH) - (278.455 \times HT^2) - (44.3675 \times HT \times SH) - (41.705 \times SH^2) \quad \text{Eq. 2}$$

$$UTS = 985.673 - (76.5283 \times HT) + (28.6133 \times SH) - (365.335 \times HT^2) - (10.875 \times HT \times SH) + (2.93 \times SH^2) \quad \text{Eq. 3}$$

$$\text{Unit Def.} = 8.14844 + (5.63933 \times HT) - (2.086 \times SH) + (5.79733 \times HT^2) - (0.72775 \times HT \times SH) + (1.44733 \times SH^2) \quad \text{Eq. 4}$$

$$\text{Max. Load} = 116.059 - (11.4233 \times HT) - (4.1 \times SH) - (40.7833 \times HT^2) + (1.835 \times HT \times SH) + (4.11667 \times SH^2) \quad \text{Eq. 5}$$

$$SHc = 0.212111 - (0.091 \times HT) - (0.136 \times SH) + (0.0153333 \times HT^2) + (0.1135 \times HT \times SH) + (0.133333 \times SH^2) \quad \text{Eq. 6}$$

$$YS = 370.393 + (13.475 \times HT) + (81.125 \times SH) - (13.475 \times HT^2) + (2.6925 \times HT \times SH) - (56.535 \times SH^2) \quad \text{Eq. 7}$$

$$UTS = 479.438 - (32.5233 \times HT) + (20.1633 \times SH) + (32.5233 \times HT^2) - (4.61 \times HT \times SH) - (16.6567 \times SH^2) \quad \text{Eq. 8}$$

$$\text{Unit Def.} = 43.7889 + (1.69833 \times HT) - (7.23167 \times SH) - (1.69833 \times HT^2) + (0.085 \times HT \times SH) + (2.29167 \times SH^2) \quad \text{Eq. 9}$$

$$\text{Max. Load} = 58.4522 - (4.90167 \times HT) - (4.28833 \times SH) + (4.90167 \times HT^2) - (0.04 \times HT \times SH) - (0.608333 \times SH^2) \quad \text{Eq. 10}$$

$$SHc = 0.312444 - (0.156333 \times HT) - (0.382833 \times SH) + (0.156333 \times HT^2) - (0.007 \times HT \times SH) + (0.273833 \times SH^2) \quad \text{Eq. 11}$$

Fig. 7 shows good agreement between the measured data and the values predicted by the statistical model's equations (Equations 2 to 11 for both materials). While correlation coefficients exceed 97% for most variables, the specific wear rate exhibits a lower value (R^2 = 84.4%). This weaker correlation for SHc can be attributed to the material chemical composition, superficial roughness, mechanical preparation, or the heat treatment applied.

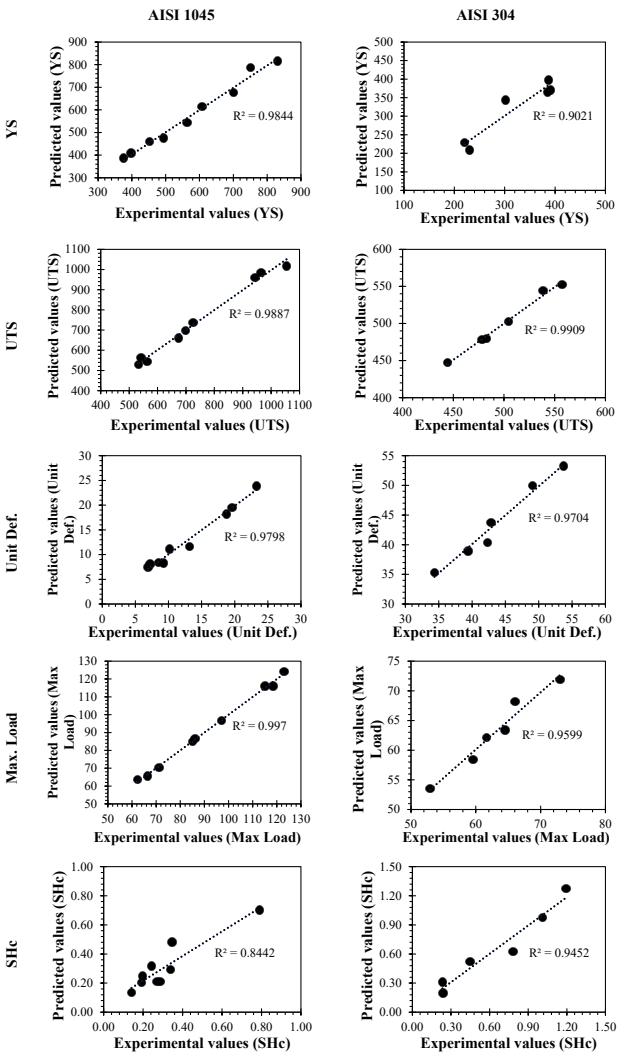

Figure 7. Estimation of calculated and measured values for both materials. Source: The authors.

1 Conclusions

Heat treatments significantly influence the mechanical properties of AISI 1045 and AISI 304 steels. Quenching AISI 1045 increases hardness by 71.9% and the stress required for strain hardening by 60.1% for 20% and 40% SH, respectively, due to martensite formation. Annealing reduces these stresses by 2.4% and 8.7% for 20% and 40% SH, respectively, allowing for stress relaxation and grain growth, which enhances ductility. In contrast, AISI 304 shows minor variations in mechanical properties after annealing, with changes of -6.9% for 20% SH and +4.4% for 40% SH, consistent with its austenitic nature.

The high R^2 values (above 0.97) for the RSM equations indicate that the predictive models are generally accurate, particularly for UTS and maximum load in AISI 304. However, the slightly lower R^2 for the SHc suggests that this property is more challenging to predict, likely due to experimental data variability or the material behavior's complexity.

The observed changes in the mechanical properties of AISI 1045 and AISI 304 after heat treatments and variations in strain hardening are consistent with the literature, showing significant increases in strength and hardness after quenching and greater ductility and energy absorption capacity after annealing. Also, strain hardening increases the yield strength of the materials by increasing dislocation accumulation, promoting the formation of new crystalline structures, and restricting the mobility of dislocations.

References

[1] Vargas-Cubillos L.F., Influencia del tratamiento térmico de recocido sobre la microestructura, dureza y atenuación ultrasónica de aceros inoxidables AISI 304, Universidad Libre, 2015.

[2] Rodríguez-Galbarro, H., Estudio y clasificación de los aceros, [online]. 2023. Available at: https://ingemecanica.com/tutorialsemanal/tutorialn101.html#google_vignette (accessed Dec. 12, 2023).

[3] Patiño-Pérez, A.P., Ortega-Breña, M., Rodríguez-Castro, R., y Ballesteros-Martínez, L., Caracterización, modelación y simulación de zona plástica para un acero de bajo contenido de carbono (AISI 1006), en: Congreso Iberoamericano de Ingeniería Mecánica, 2017, pp. 1–9.

[4] Salman, K.D., Microstructure and mechanical properties of cold rolled AISI 1018 Low Carbon Steel, IOP Conf. Ser. Mater. Sci. Eng., 551(1), art. 12007, 2019. DOI: https:// doi.org/10.1088/1757-899X/551/1/012007.

[5] Dimatteo, A., Colla, V., Lovicu, G., and Valentini, R., Strain hardening behavior prediction model for automotive high strength multiphase steels, Steel Res. Int., 86(12), pp. 1574–1582, 2015. DOI: https://doi.org/10.1002/srin.201400544.

[6] Bounezour, H., Laouar, L., Bourbia, M., and Ouzine, B., Effects of work hardening on mechanical metal properties—experimental analysis and simulation by experiments, Int. J. Adv. Manuf. Technol., 101(9), pp. 2475–2485, 2019. DOI: https://doi.org/10.1007/s00170-018-3071-x.

[7] Eom, J.G. et al., Effect of strain hardening capability on plastic deformation behaviors of material during metal forming, Mater. Des., 54, pp. 1010–1018, 2014. DOI: https://doi.org/10.1016/j.matdes.2013.08.101.

[8] Perez, W., Olaya, J.J., and Arenas, J.A., Influence of conditions of heat treatment on the mechanical properties of steel 5160H, Rev. Técnica la Fac. Ing. Univ. del Zulia, [Online]. 36(1), pp. 23–31, 2013. Available at: https://ve.scielo.org/scielo.php?script=sci_arttext&pid=S0254-07702013000100004&nrm=iso.

[9] Toribio, J. et al., Analysis of the bauschinger effect in cold drawn pearlitic steels, metals, 10(1), art. 10114, 2020. DOI: https://doi.org/10.3390/met10010114.

[10] Soria-Aguilar, M. de J. Efecto del tratamiento térmico sobre las propiedades mecánicas y microestructura de un acero para tubería API 5CT J55, Ing. Investig. y Tecnol., 16(4, pp. 539–550, 2015. DOI: https://doi.org/10.1016/j.riit.2015.09.006.

[11] Alexander P.W., y William, R.R., Análisis de las propiedades mecánicas de tensión, tenacidad y dureza de un acero SAE 1045 mediante los procesos de tratamiento térmico de temple, criogenia y revenido, Universidad Distrital Francisco José de Caldas, 2017.

[12] Vaca-Ortega, W.H., and Guerrero-Lara, E.S., Estudio de los tratamientos térmicos en el acero AISI 1045 en un sistema acuoso evaluados con la norma ASTM G105-89 que permitirá determinar la velocidad de desgaste del material, Universidad Técnica de Ambato, 2015.

[13] ASTM-E8/E8M, Standard test methods for tension testing of metallic materials 1, Annu. B. ASTM Stand. 4(C), pp. 1–27, 2010. DOI: https://doi.org/10.1520/E0008.

[14] García-León, R.A. et al., Effect of heat treatments on the strain hardening behavior of AISI 1045 and 304 Steels, J. Mater. Eng. Perform., pp. 1–16, 2024. DOI: https://doi.org/10.1007/s11665-024-10251-w.

[15] UAB, VII Endurecimiento por deformación y recocido, Universidad de Chile, Santiago de Chile, 2015.

[16] Afrin, N., Chen, D.L., Cao, X., and Jahazi, M., Strain hardening behavior of a friction stir welded magnesium alloy, Scr. Mater., 57(11), pp. 1004–1007, 2007. DOI: https://doi.org/10.1016/j.scriptamat.2007.08.001.

[17] García-León R.A. et al., Dry sliding wear test on borided AISI 316L stainless steel under ball-on-flat configuration: a statistical analysis, Tribol. Int., 157(May), art. 106885, 2021. DOI: https://doi.org/10.1016/j.triboint.2021.106885.

[18] García-León, R.A., Afanador-García, N., and Gómez-Camperos, J.A., Mechanical and dynamic maps of disc brakes under different operating conditions, Fluids, 6(10), art. 100363, 2021. DOI: https://doi.org/10.3390/fluids6100363.

[19] Statgraphics, Diseño de Experimentos –Diseños de Mezclas, Biblioteca Statgraphics, [online]. 2006. Available at: https://www.statgraphics.net/tutoriales/.

[20] Montgomery, D., and Runger, G., Applied statistics and probability for engineers, WILEY. United States of America, 2018.

[21] Singh, K.K., Strain hardening behaviour of 316L austenitic stainless steel, Mater. Sci. Technol., 20(9), pp. 1134–1142, 2004. DOI: https://doi.org/10.1179/026708304225022089.

[22] Hung, T.-P., Shi, H.-E., and Kuang, J.-H., Temperature modeling of AISI 1045 steel during surface hardening processes, Materials, 11(10), art. 101815, 2018. DOI: https://doi.org/10.3390/ma11101815.

[23] Garzón-Torres, J.R., Bohórquez-Avila, C.A., Hernandez, M.E., and Rojas-Molano, H.F., Influencia en las propiedades mecánicas del acero AISI-SAE 1045 tratado térmicamente con temple a temperatura intercrítica y revenido, Av. Investig. en Ing., 13(1) SE-Artículos, 2016. DOI: https://doi.org/10.18041/1794-4953/avances.2.257.

[24] Moghanizadeh, A., and Farzi, A., Effect of heat treatment on an AISI 304 austenitic stainless steel evaluated by the ultrasonic attenuation coefficient, 58(5), pp. 448–452, 2016. DOI: https://doi.org/10.3139/120.110878.

[25] Essoussi, H., Elmouhri, S., Ettaqi, S., and Essadiqi, E., Heat treatment effect on mechanical properties of AISI 304 austenitic stainless steel, Procedia Manuf., 32, pp. 883–888, 2019. DOI: https://doi.org/10.1016/j.promfg.2019.02.298.

R.A. García-León, received the BSc. Eng. in Mechanical Engineering in 2014, from the Universidad Francisco de Paula Santander Ocaña, Colombia. Sp., MSc. and PhD. Scientist in Mechanical Engineering from the Instituto Politecnico Nacional. Professor in the engineering Faculty of the Universidad Francisco de Paula Santander, Ocaña, and Universidad del Magdalena, Santa Marta, Colombia. Researcher in the INGAP and GIS Research Groups. His areas of interest are mainly mechanical systems, design, industrial processes, engineering materials, wear and tribology.
ORCID: 0000-0002-2734-1425

H.Y. Jaramillo, a BSc. in Civil Construction in 2007, with Sp. in Civil Works Supervision and projects in 2009, and a MSc. in Construction with an emphasis in sustainability in 2014, all of them from the Universidad Nacional de Colombia, Medellin, has worked in the construction sector in public and private projects and has served as a teacher in different universities of the city of Medellin from 2009 - 2017 and currently teacher in the Civil Engineering Department at the Francisco de Paula Santander University, in Ocaña, Colombia. His research interests are in the field of ecomaterials and sustainability in all aspects of engineering and construction.
ORCID: 0000-0002-4185-119X

J. Gómez-Camperos, received the BSc. Eng. in Mechatronic Engineering from the Universidad de Pamplona, Colombia, in 2007. Msc. in Industrial Controls of the same University. Full-time teacher in the Department of Mechanical Engineering of the Faculty of Engineering of the Universidad Francisco de Paula Santander, Ocaña, Colombia from 2018. Also, is the director of the research group in new technologies, sustainability, and innovation (GINSTI).
ORCID: 0000-0003-3894-144X